PROCEEDINGS, TOUGH Symposium 2003
Lawrence Berkeley National Laboratory, Berkeley, California, May 12–14, 2003

ESTIMATING FLOW PARAMETERS USING GROUND-PENETRATING RADAR AND HYDROLOGICAL DATA DURING TRANSIENT FLOW IN THE VADOSE ZONE

Michael Kowalsky[1], Stefan Finsterle[2], and Yoram Rubin[1]

[1]Dept. of Civil and Environmental Engineering, University of California, Berkeley
Berkeley, CA 94720, USA
e-mail: MBKowalsky@lbl.gov

[2]Earth Sciences Division, Lawrence Berkeley National Laboratory
Berkeley, CA 94720, USA

ABSTRACT

Methods for determining the parameters necessary for modeling fluid flow and contaminant transport in the shallow subsurface are in great demand. Soil properties such as permeability, porosity, and water retention are typically estimated through the inversion of hydrological data (e.g., measurements of capillary pressure and water saturation). However, ill-posedness and non-uniqueness commonly arise in such inverse problems making their solutions elusive. Incorporating additional types of data, such as from geophysical methods, may greatly improve the success of inverse modeling. In particular, ground-penetrating radar (GPR) has proven sensitive to subsurface fluid flow processes. In the present work, an inverse technique is presented in which permeability distributions are generated conditional to time-lapsed GPR measurements and hydrological data collected during a transient flow experiment. Specifically, a modified pilot point framework has been implemented in iTOUGH2 allowing for the generation of permeability distributions that preserve point measurements and spatial correlation patterns while reproducing geophysical and hydrological measurements. Through a numerical example, we examine the performance of this method and the benefit of including synthetic GPR data while inverting for fluid flow parameters in the vadose zone. Our hypothesis is that within the inversion framework that we describe, our ability to predict flow across control planes greatly improves with the use of both transient hydrological measurements and geophysical measurements (GPR-derived estimates of water saturation, in particular).

INTRODUCTION

Predicting how quickly a spilled contaminant will migrate through the vadose zone and into an aquifer, or predicting water availability for crops at root zones, for example, depends on soil properties such as permeability, porosity, and water retention. Techniques are available for measuring point values of these fluid flow parameters directly in the field or using soil cores in the laboratory. However, fluid flow parameters are commonly heterogeneous, and uncertainty in their spatial distributions makes it difficult to model fluid flow and contaminant transport from point measurements alone. Furthermore, point measurements are commonly limited due to their collection being expensive, time consuming, and invasive (with the potential for creating preferential flow paths). Techniques allowing for the inference of flow parameter distributions are, therefore, in high demand.

In some cases, when spatial statistics at a given site are known, conditional simulation techniques may be used to generate parameter fields in which point measurements and spatial correlation patterns are preserved. However, fields generated with such techniques do not, in general, accurately predict flow. Parameter inversion techniques are typically required for this purpose.

The development of inverse techniques has allowed for the estimation of flow parameters given both point measurements and hydrological data. While substantial progress has been made in accounting for multi-dimensional spatially heterogeneous flow properties in the saturated zone, inverse methods for the vadose zone are less common and have mostly involved one-dimensional cases, usually uniform or layered soil columns (e.g., Kool et al., 1985; Simunek and van Genuchten, 1996; Zhou et al., 2001). This is in large part due to the difficulty in overcoming ill-posedness and non-uniqueness inherent to such problems. One way to make inverse problems more amenable to solution is by including additional types of data. Incorporating geophysical measurements, in particular, into inverse techniques for the vadose zone is a promising area of research (e.g., Hubbard et al., 1997; Binley et al., 2002; Yeh et al., 2002), though still in its infancy.

Generally stated, the inverse problem may be defined as estimating a set of relevant flow parameters given: 1) point measurements of the flow parameters, 2) some hydrological measurements collected during a flow experiment, along with 3) any other (possibly transient) measurements that are sensitive to flow processes, including geophysical measurements. A

solution to this inverse problem results in a parameter distribution for which the simulated and measured observational data match (assuming that adequate models exist for simulating each data type), and the parameter measurements are preserved.

In the present study, we assume that the absolute permeability is the only non-uniform and unknown flow parameter, and that its log value is a randomly varying field characterized by a log-normal distribution with known spatial correlation patterns. Through inversion, we attempt to approximate the absolute permeability field using various combinations of measurements including: point measurements of permeability; measurements of water saturation in the boreholes (attainable by methods such as neutron probe logging); and horizontally averaged water saturation values (attainable from zero-offset profile GPR measurements). Additional types of data, including capillary pressure and flux measurements, can also be easily included in the method we describe.

PROBLEM STATEMENT

For the current study, observational data are generated for a known model to obtain the measurement vector $\mathbf{z}_{meas} = [\mathbf{z}^{sat}_{meas}, \mathbf{z}^{GPR}_{meas}]$, where $\mathbf{z}^{sat}_{meas}$ and $\mathbf{z}^{GPR}_{meas}$ are the borehole saturation and GPR measurements (both collected in different locations for numerous times), respectively. The measurement error vector **v** is defined as the difference between the true and measured observation data. A vector of unknown log permeability values is given by **a**, which, after being mapped to the entire flow domain, allows for the simulation of observational data $\mathbf{z}_{sim} = [\mathbf{z}^{sat}_{sim}, \mathbf{z}^{GPR}_{sim}]$, where the subsets of borehole saturation and GPR data types are similarly denoted as for $\mathbf{z}_{meas}$.

Both **a** and **v** are assumed to be independent Gaussian distributions with known covariance matrices C_a and C_v, respectively. Therefore, for estimating **a**, the objective function (OF) derived from the Gaussian maximum a posteriori formulation (e.g., McLaughlin and Townley, 1996) may be used. It is given by

$$OF(\mathbf{a}) = [\mathbf{z}_{meas} - \mathbf{z}_{sim}]^T \mathbf{C}_{\mathbf{v}}^{-1} [\mathbf{z}_{meas} - \mathbf{z}_{sim}] + [\mathbf{a} - \bar{\mathbf{a}}]^T \mathbf{C}_{\mathbf{a}}^{-1} [\mathbf{a} - \bar{\mathbf{a}}] \quad (1)$$

where $\bar{\mathbf{a}}$ is a prior estimate of **a**. The first term in (1) represents the mismatch between measured and simulated observations for **a**, and the second term represents the mismatch between **a** and its prior values. Finding a set of parameters **a** that minimizes (1) defines the inverse problem for the present study.

METHODOLOGY

The estimation of **a**, given the measurements described above, is made possible through inversion with concepts from the pilot point method. A means for mapping the discrete values of **a** to the entire flow domain, such as through sequential simulation (e.g., Deutsch and Journel, 1992), makes this possible. An overview of the pilot point method is given next, followed by a description of our implementation of the method, and a brief description of the optimization technique employed.

Pilot Point Framework

The pilot point method was originally developed in work such as Marsily (1984) and Certes and Marsily (1991). The essence of the method lies in: 1) generating a fluid flow parameter field that honors parameter measurements (usually using sequential simulation), and then 2) perturbing the field in select locations to obtain a better match between measured and simulated observational data, while 3) preserving known spatial correlation patterns. The set of points that parameterizes the field are called pilot points, and their values are estimated through inversion. Application of the method, including how perturbations are propagated throughout the field, how pilot point locations are chosen, which observational data are used, and details regarding the objective function (e.g., weighting of parameters, observational data, and prior information) differ greatly among previous implementations of the method.

While some of the perceived benefit of early work on the pilot point method derived from its flexibility in choosing pilot point locations, later innovative work involved finding more systematic and efficient approaches for positioning pilot points. RamaRao et al. (1995) proposed a method for adding pilot points sequentially, after finding their optimal locations with adjoint sensitivity analyses. Some concerns were later raised regarding the addition of pilot points in this manner (Cooley, 2000). In an alternate implementation given by Gomez-Hernandez et al. (1997), pilot points were placed on a pseudo-regular grid and called master points, and inversion for their values was performed simultaneously. They found the optimal master point spacing to be on the order of 2 to 3 points per correlation length.

The pilot point framework is well suited for inclusion of different data types under varied flow conditions. Much of the work mentioned above involved horizontal flow in the saturated zone, where the parameter of interest was the log transmissivity, and observational data included steady-state and transient piezometric measurements. Wen et al. (2002) extended the method of Gomez-Hernandez et al. (1997) to include transient tracer data, and found in a

synthetic study that the combination of (noise-free) piezometric head and tracer data improved their ability to predict transport.

In previous work, prior information for pilot points was most commonly implemented through parameter constraints (i.e., pilot points were allowed to vary freely within strict bounds around the initial values or the kriging estimates (e.g., Certes and Marsily, 1991; RamaRao et al., 1995; Gomez-Hernandez et al., 1997). This is equivalent to constrained minimization of (1) without the second term, and with the error covariance matrix C_v being represented by some relative weighting parameter—though it was often assumed that there was zero measurement/estimation error. The inclusion of prior pilot point information using a "Gaussian regularization term" was suggested as a potential improvement to the method (McLaughlin and Townley, 1996). This is equivalent to minimizing the objective function given in (1).

Proposed Implementation

In the present work, we consider the case of a vadose zone model in which the log of the absolute permeability is an unknown stochastic field, and the remaining flow parameters (e.g., the porosity and the parameters describing the relative permeability and capillary pressure functions) are considered known and constant. (Note: For simplicity, absolute permeability will subsequently be referred to as permeability.) We also assume that the possibly anisotropic correlation function (or semi-variogram) describing the log permeability distribution is known (e.g., from an outcrop study). If available, permeability measurements are assumed to be from a support scale equal to that of the grid blocks at which flow is modeled and their error distributions known. In addition, the measurement error distributions are Gaussian with zero mean and known variance.

The objective function we use in this work is given in (1), where each the diagonal elements of the pilot point covariance matrix are the calculated kriging variance values (and the off-diagonal elements of the matrix are zero), and the prior values of the pilot points are taken to be the kriging estimates. If no measurements are available, then the kriging estimates of the prior and the variance equal the population mean and variance, respectively (i.e., as prior values become more accurate, more weight is given to them).

Since the goal of the method is to predict flow phenomena (rather than to obtain a smooth model that represents an average of all possible models), implementation requires multiple inversions with different random field realizations (each with a different seed number). Each of the resulting models is plausible and equally likely given the available data. For increasingly well-designed problems, fewer realizations are required.

For a given realization, a parameter field is generated, and the set of parameters (pilot points), whose locations are defined prior to inversion are estimated simultaneously through inversion. (Note that although there are similarities with this implementation to that of Gomez-Hernandez et al. (1997), we will refer to the unknowns as pilot points rather than master points). Inversion involves perturbing values at these points, re-generating the parameter field using sequential simulation (in essence propagating the perturbations throughout the parameter field), simulating flow and GPR with the perturbed field, and then evaluating the objective function. The final model is the model with minimal deviation from the prior distribution for which measured and simulated observational data match best (i.e., the model which minimizes (1)).

Implementation details

The method we propose here has recently been implemented in iTOUGH2 (Finsterle, 1999), a code that provides inverse modeling capabilities to the TOUGH2 flow simulator (Pruess et al., 1999). An outline of the steps in the procedure is as follows:

1) Measurements are collected in a field test (or synthetic data are generated for synthetic study).
2) The number and locations of pilot points are defined.
3) For a given realization (random field seed number), a log permeability field **a** is generated. This field is modified in steps 5-6.
4) Simulated measurements $\mathbf{z}_{sim}$ are generated, and used to calculate the initial value of the objective function for this realization.
5) Pilot point values are perturbed via an optimization algorithm (described in the next section), and a new field (with the same seed number) is generated using the newly perturbed values. The pilot points are treated as data points in the sequential simulation such that the perturbation of a pilot point value is propagated throughout the region near that point, the extent of influence depending on the correlation range of the model.
6) Simulated measurements $\mathbf{z}_{sim}$ are generated with the perturbed field obtained from (5), and used to calculate the new value of the objective function.
7) Steps 5 – 6 are repeated until the solution for this realization is found.
8) Steps 3 – 7 are repeated for multiple realizations (different seed numbers).

Optimization algorithm

The success of any inversion depends on the careful choice and implementation of optimization algorithm. Parameter inversion methods are most commonly performed using gradient based methods (e.g., the Levenberg-Marquardt technique). But, because of the complex nature of inverse problems in the vadose zone, the use of non-gradient methods for these applications has also been suggested (Pan and Wu, 1998). While usually less efficient than gradient-based methods, non-gradient methods such as Simulated Annealing and Downhill Simplex are robust, less sensitive to initial conditions, and require no assumptions to be made about the objective function, such as it being quadratic or smooth (Pan and Wu, 1998).

For the example shown next, we found the application of gradient-based methods to be unstable. However, optimization using the Downhill Simplex method was found to work suitably. Following convergence during the inversion for each realization, optimization was reinitialized using the just-obtained parameters as initial guesses with an increased simplex size. This helped to ensure identification of the global minimum. Details of the Downhill Simplex method and its implementation are not given here but have been well documented elsewhere (e.g., Nelder and Mead, 1965; Press, et al., 1992).

NUMERICAL EXAMPLE

Ponding Experiment

Here we consider a two-dimensional vadose zone model extending 3 meters deep and 4 meters in the horizontal direction with 10 cm nodal spacing in the vertical and horizontal directions. The saturation values of the upper boundary of the model are allowed to vary during an infiltration test, but are considered to be known. To represent the water table, saturation values along the lower boundary of the model are kept fully saturated. The vertical sides of the model are treated as no-flow boundaries. See Figure 1 for a schematic of the model.

The soil properties of the model (i.e., the relative permeability and capillary pressure functions), are described by a commonly used parametric formulation (van Genuchten, 1980). As mentioned above, all of the parameters characterizing the soil properties are known and constant except for the absolute permeability, which is a spatially correlated stochastic field. (Note that the capillary pressure is scaled with permeability according to the convention of Leverett (1941).) Specifically, an absolute permeability field was generated using sequential Gaussian simulation (SGSIM) (Deutsch and Journel, 1992). This field, shown in Figure 2a, was generated using an anisotropic Gaussian correlation function with effective horizontal and vertical ranges of 1.5 m, and 0.75 m, respectively, and with a variance of 0.5 m^2, and a nugget value of 0.01 m^2.

After simulating gravity-capillary equilibrium (with uniform water saturation of 0.3 at the surface), a ponding infiltration experiment was simulated by imposing fully saturated conditions over a 1 meter region on the surface (see Figure 1) for 4 hours. Following that, the surface was returned to pre-infiltration conditions.

Synthetic Observations

Hydrological and geophysical measurements were simulated during the ponding experiment and were, thereafter, considered to be the measured data. For this purpose, two boreholes were "placed" in the left and right sides of the model (at horizontal positions of 1 and 3 meters, respectively, in Figure 1) extending from the surface to the water table. Permeability measurements were taken from each borehole at 30 cm spacing (with each measurement corresponding to the same support volume used in the flow modeling) giving 20 point measurements. Water saturation measurements were also taken in each borehole at 20 depths (between -0.1 m and -2.1 m, with a 10 cm interval) at 35 points in time over a period of 12 hours. Measurement error was generated from a zero-mean normal distribution (with variance equal to 0.01) and added to the synthetic water saturation measurements.

In addition, we wish to evaluate the potential benefit of including crosshole GPR measurements in the flow inversion. In crosshole GPR applications, high-frequency electromagnetic (EM) pulses are propagated from one borehole to another for various antenna configurations. In the present study, zero-offset profile (ZOP) measurements, in particular, are considered. To obtain a ZOP data set, the source and receiver antennas are moved incrementally, while being kept at equal depths, such that transmitted waveforms may be recorded at each depth. In some cases, since the travel times of the EM pulses are affected by water saturation, they may be used as observational data for flow inversion. Alternatively, the travel times may be converted to EM wave velocity, and then to dielectric constant, which, when the soil porosity is known, may be converted to water saturation through a petrophysical model (e.g., Roth et al., 1990). A water saturation profile derived from a ZOP data set represents a depth profile of the horizontally averaged inter-borehole water saturation values at a given time.

For the present study, horizontally averaged water saturation values are calculated within iTOUGH2 for each time as a proxy for simulated ZOP measurements. This was partly justified by considering that

water saturation profiles derived from simulations with a GPR finite difference code match pseudo-GPR profiles calculated in iTOUGH2 (not shown). Measurement error was also added to the pseudo-GPR measurements through a zero-mean normal distribution (with variance equal to 0.01).

Inversion with Different Data Types

The inversion procedure is now evaluated for several combinations of data types and compared to models obtained through conditional simulation. Figure 2b shows a log permeability field generated conditional to some permeability point measurements (at locations indicated with black dots). The model obtained through inversion of the GPR measurements alone is shown in Figure 2c. Figure 2d shows the model obtained through inversion using GPR and borehole saturation measurements. For the cases where inversions were performed, (c) and (d), the pilot point locations are indicated by open circles, and the observational measurement locations are marked with open squares (the pseudo-GPR measurements measure the average water saturation between the two open squares at each depth).

Note that the measured permeability values from (a) are preserved in each of the models shown in (b) – (d). Also note that while the same seed number was used for obtaining these models, a different seed number was used for generating the true model (a).

The model obtained with borehole saturation and GPR measurements (d) appears to best reproduce the true model (a) in the region between the boreholes. For example, both models show a high permeability zone at the horizontal position of 1.5m and the depth of -0.7m. However, deviation from the true model is seen between the true model and all other models in the region below -2m (including between the boreholes), where no observation data were collected.

How well the models in (b) – (d) predict the observational data (water saturation in the left and right boreholes, and that derived from the pseudo-GPR measurements) is shown in Figure 3. For the first case, none of the observational data were used to obtain the model, and the mismatch between measured and predicted observations is large (Figure 3a). For the second case mentioned above, the GPR measurements alone were used in the inversion, and the measured GPR values are predicted, though the measured borehole saturation values are not (Figure 3b). For the third case, both data types were used in the inversion, and the values in each synthetic data set are well predicted (Figure 3c).

Inversion Performance

Performance of the inversion procedure is now evaluated by comparing the real breakthrough curves at several control planes (depicted in Figure 1) with the breakthrough curves generated using the various models. Two additional cases are included which were not described above: an unconditional simulation (using no permeability measurements), and an inversion using only borehole saturation measurements. Figure 4 shows that both unconditionally and conditionally simulated models fail to consistently predict breakthrough at each of the control planes. Inversion with borehole saturation values improves the prediction, but not as much as adding GPR measurements. Adding either GPR or both GPR and borehole saturation measurements gives similarly good predictions. Note that for the best cases, predictions at the lowest control plane (CP 3, as labeled in Figure 1) are less accurate than for the upper two control planes.

When considering lateral variation in breakthrough curves, different conclusions are drawn regarding the benefit of GPR measurements. Predictions from conditional simulations remain inaccurate (Figure 5a). However, better predictions are obtained when using both GPR and borehole saturation measurements together versus using GPR measurements alone (compare Figure 5b and Figure 5c).

CONCLUSIONS

Inversion with synthetic data indicates that different measurement types, including transient hydrological and geophysical (namely GPR), allow for good prediction of flow phenomena. Simulated pseudo-GPR measurements alone were seen to accurately predict total breakthrough at several control planes. However, to predict lateral variations in breakthrough at the control planes, the combination of GPR measurements with borehole water saturation values was found to work best.

Prediction at the lowest control plane was poorest. This is because improvements to initial realizations are limited in regions without pilot points or observational measurements, like in the region below -2 m depth.

Future work includes the investigation of various GPR measurement configurations (other than ZOP), antenna frequencies (which determine the averaging volume for water saturation estimates) and temporal sampling strategies (i.e., how often GPR surveys are collected). These issues will be more accurately investigated when GPR finite difference modeling is implemented in iTOUGH2.

ACKNOWLEDGMENT

Thanks are due to Christine Doughty and Seiji Nakagawa for their careful reviews of the manuscript. This work was supported by the U.S. Dept. of Agriculture NRI grant 2001-35102-09866 Ground-Penetrating Radar: Development of a Vineyard Management Tool, and by U.S. Dept. of Energy under Contract No. DE-AC03-76SF00098.

REFERENCES

Binley, A., G. Cassiani, R. Middleton, P. Winship, Vadose zone flow model parameterization using cross-borehole radar and resistivity imaging, *J. of Hydrology*, 267, 147-159, 2002.

Certes, C., and G. de Marsily, Application of the pilot point method to the identification of aquifer transmissivities, *Adv. Water Resour.*, 14(5), 284-300, 1991.

Cooley, R. L., An analysis of the pilot point methodology for automated calibration of an ensemble of conditionally simulated transmissivity fields, *Water Resour. Res.*, 36(4), 1159-1164, 2000.

Deutsch, C.V., and A.G. Journel, GSLIB: Geostatistical Software Library and User's Guide, Oxford Univ. Press, New York, 1992.

Finsterle, S., iTOUGH2 User's Guide. Report LBNL-40040. Lawrence Berkeley National Laboratory, Berkeley, CA, 1999.

Gomez-Hernandez, J. J., A. Sahuquillo, J. E. Capilla, Stochastic simulation of transmissivity fields conditional to both tranmissivity and piezometric data—1. Theory, *J. of Hydrology*, 203, 162-174, 1997.

Hubbard, S.S., Rubin, Y. and Majer, E., 1997, Ground-penetrating-radar-assisted saturation and permeability estimation in bimodal systems: *Water Resour. Res.*, 33(5), p. 971-990.

Kool, J. B., J. C. Parker, M. T. van Genuchten, Determining soil hydraulic properties from one-step outflow experiments by parameter estimation, I, Theory and numerical studies, *Soil Sci. Soc. Am. J.*, 49, 1348-1354, 1985.

Leverett, M.C., Capillary Behavior in Porous Solids: Trans. Soc. Pet. Eng. AIME, 142, 152-169, 1941.

de Marsily, G., Spatial variability of properties in porous media: A stochastic approach, in Fundamentals of Transport in Porous Media, eds. J. Bear and M. Y. Corapcioglu, 719-769, Martinus Nijhoff, Boston, 1984.

McLaughlin, D., and L. R. Townley, A reassessment of the groundwater inverse problem, *Water Resour. Res.*, 32(5), 1996.

Nelder, J. A., and R. Mead, A simplex method for function minimization, *Comput. Journal*, 7, 308-313, 1965.

Pan, L., and L. Wu, A hybrid global optimization method for inverse estimation of hydraulic parameters: Annealing-simplex method, *Water Resour. Res.*, 34(9), 2261-2269, 1998.

Press, W. H., S. A. Teukolsky, W. T. Vetterling, and B. P. Flannery, Numerical Recipes in Fortran, 2nd. ed., Cambridge Univ. Press, New York, 1992.

Pruess, K., C. Oldenburg, and G. Moridis, *TOUGH2 User's Guide, Version 2.0*, Report LBNL-43134, Lawrence Berkeley National Laboratory, Berkeley, Calif., 1999.

Ramarao, B. S., A. M. LaVenue, G. de Marsily, M. G. Marietta, Pilot point methodology for automated calibration of an ensemble of conditionally simulated transmissivity fields, 1, Theory and computational experiments, *Water Resour. Res.*, 31(3), 475-493, 1995.

Roth, K.R., R. Schulin, H. Fluhler, and W. Attinger, Calibration of time domain reflectometry for water content measurement using a composite dielectric approach, *Water Resour. Res.*, 26, 2267-2273, 1990.

Simunek, J., and M.T. van Genuchten, Estimating soil hydraulic properties from tension disc infiltrometer data by numerical inversion, *Water Resour. Res.*, 32(9), 2683-2696, 1996.

van Genuchten, M. Th., A closed-form equation for predicting the hydraulic conductivity of unsaturated soils: *Soil. Sci. Soc. Am. J.*, 44, 892-898, 1980.

Wen, X. -H., C. V. Deutsch, and A. S. Cullick, Construction of geostatistical aquifer models integrating dynamic flow and tracer data using inverse technique, *J. of Hydrology*, 255, 151-168, 2002.

Yeh, T.-C., S. Liu, R. J. Glass, K. Baker, J. R. Brainard, D. Alumbaugh, and D. LaBrecque, A geostatistically based inverse model for electrical resistivity surveys and its applications to vadose zone hydrology, *Water Resour. Res.*, 38(12), 1278, 2002.

Zhou, Z.-Y., M. H. Young, Z. Li, and P. J. Wierenga, Estimation of depth averaged unsaturated soil hydraulic properties from infiltration experiments, *J. of Hydrology*, 242, 26-42, 2001.

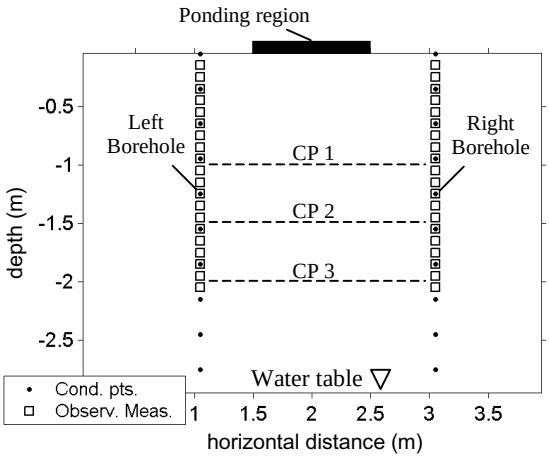

Figure 1. Vadose zone model used in numerical example. Boreholes are located at horizontal positions of 1 m and 3 m. Permeability measurements are taken from each borehole at 30 cm spacing (shown as black dots), water saturation measurements are taken in the boreholes (at open squares), and the pseudo-GPR measurements represent horizontally averaged water saturation values between the boreholes (between open squares). Control planes used to test inversion performance are denoted by CP 1, CP 2, and CP 3.

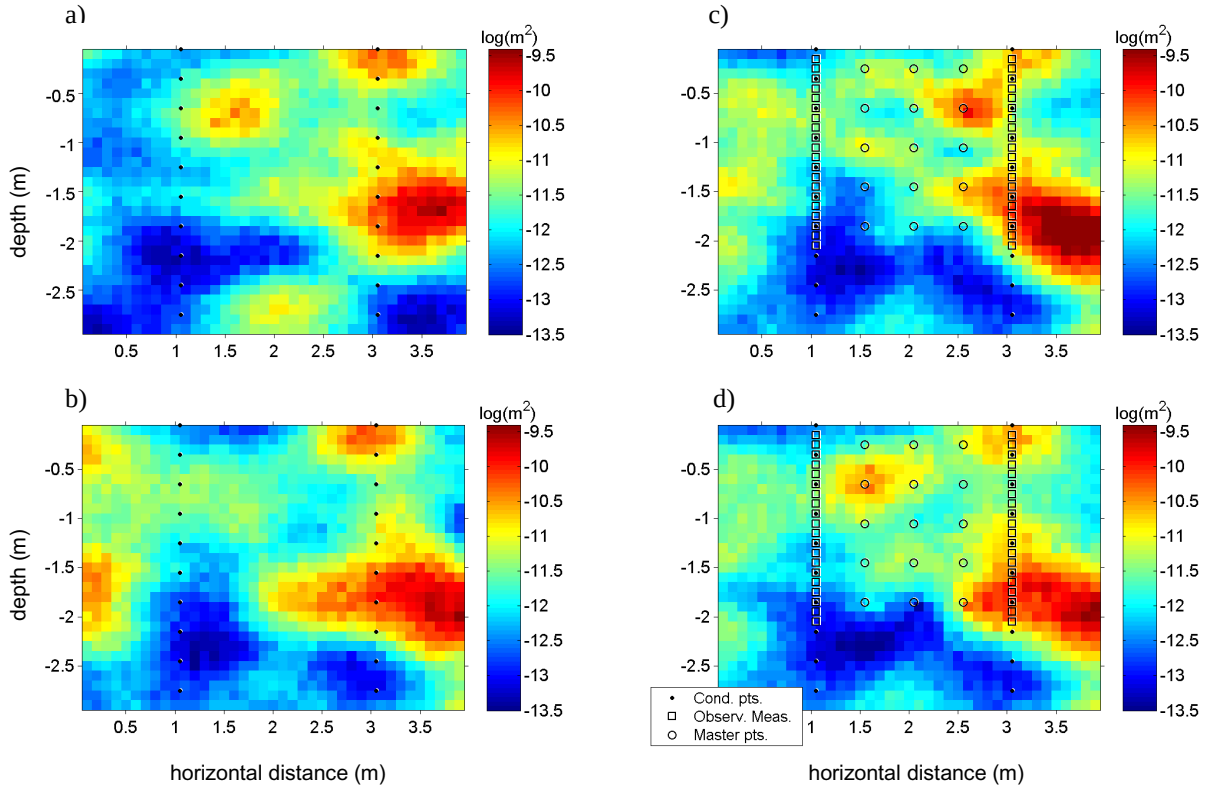

Figure 2. Models of absolute permeability: a) used to generate synthetic observations during a ponding experiment; b) obtained through conditional simulation; c) obtained through inversion using synthetic GPR measurements; and d) obtained through inversion using synthetic GPR and borehole saturation measurements. The ponding region is indicated in Figure 1.

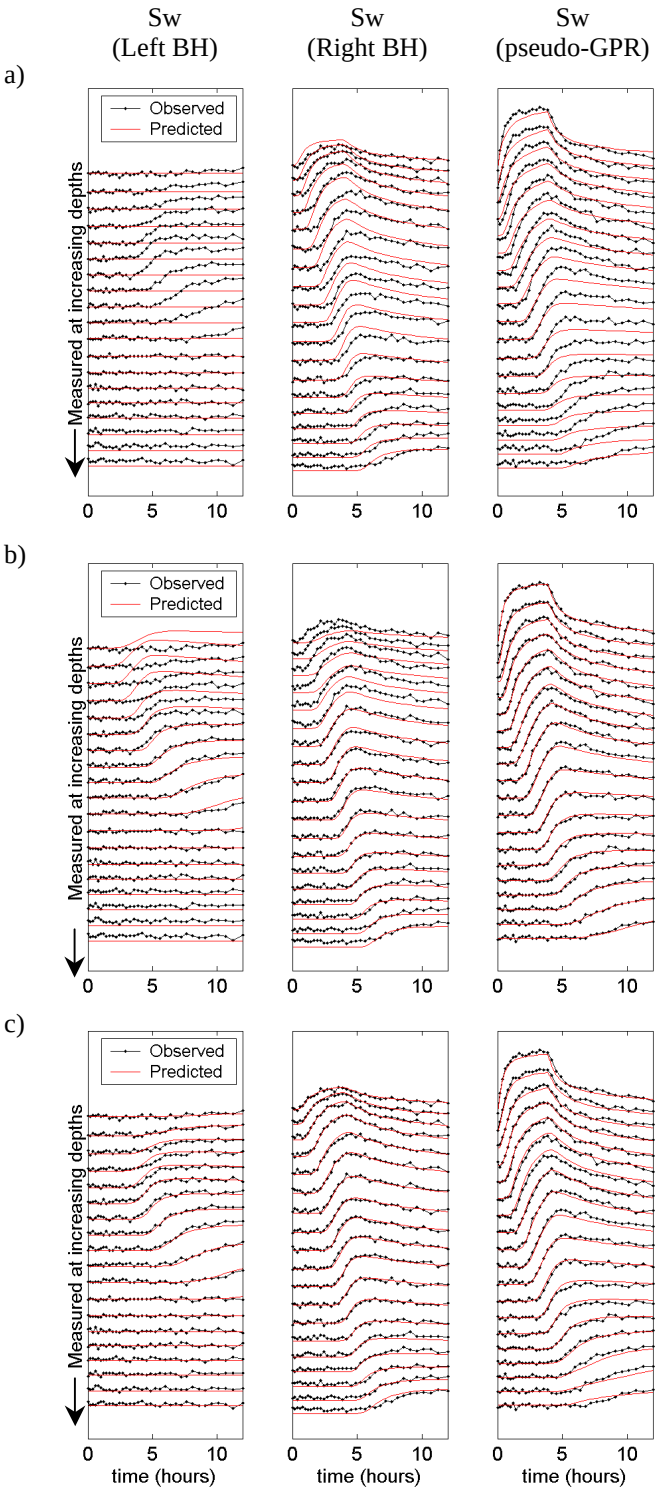

Figure 3. Misfit between simulated (shown with black dotted lines) and predicted (shown with red lines) water saturation in left borehole (1st column), right borehole (2nd column), and horizontally averaged water saturation from pseudo-GPR measurements (3rd column) for one realization. Three cases are shown: a) conditional simulation, b) inversion using synthetic GPR measurements and c) inversion using synthetic GPR and borehole saturation measurements.

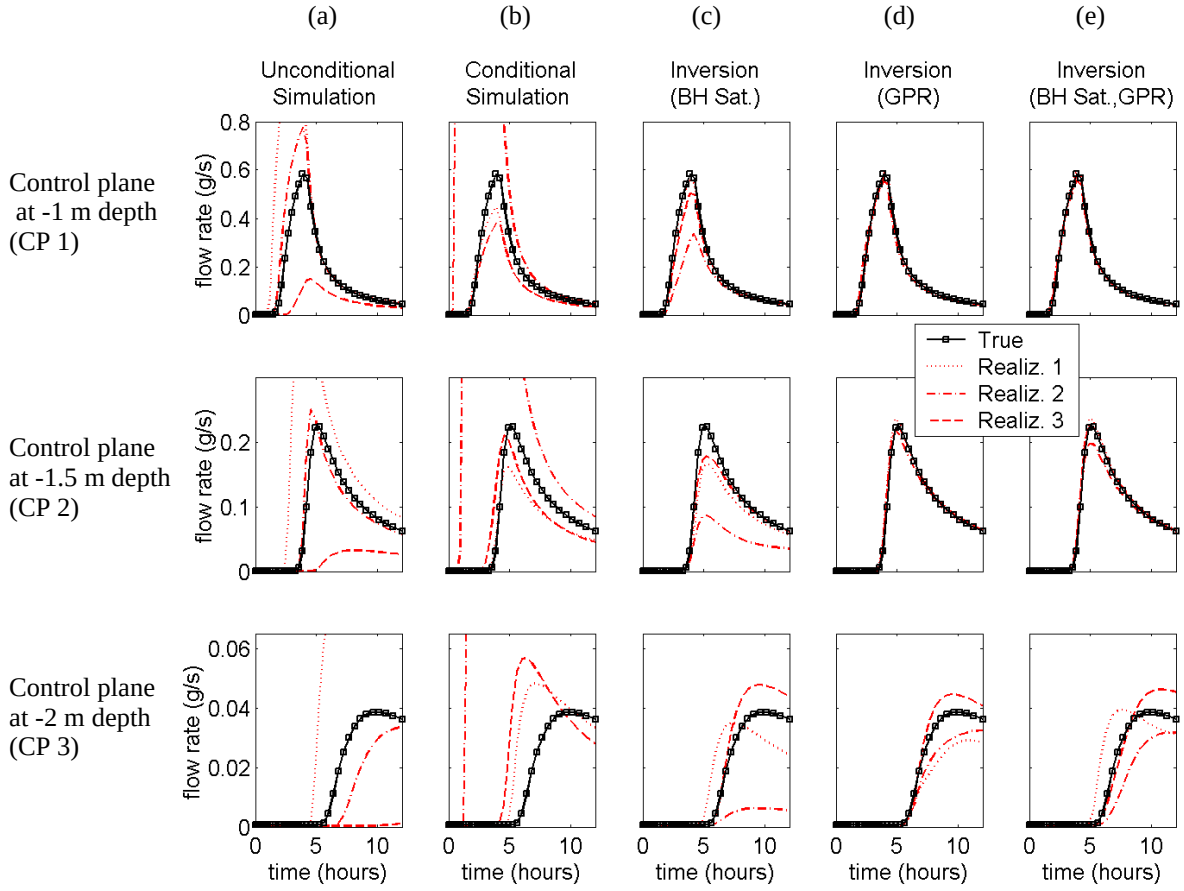

Figure 4. Breakthrough curves (total flow rates) at three control planes CP 1, CP 2, and CP 3 (as defined in Figure 1) for these cases: unconditional simulation (column a); conditional simulation (column b); inversion with left and right borehole saturation values (column c); inversion with only GPR (column d); and inversion with GPR along with left and right borehole saturation values (column e). Breakthrough for the true model is shown with black squares, and breakthrough for inversion using three different seed numbers (representing three realizations) are shown in red.

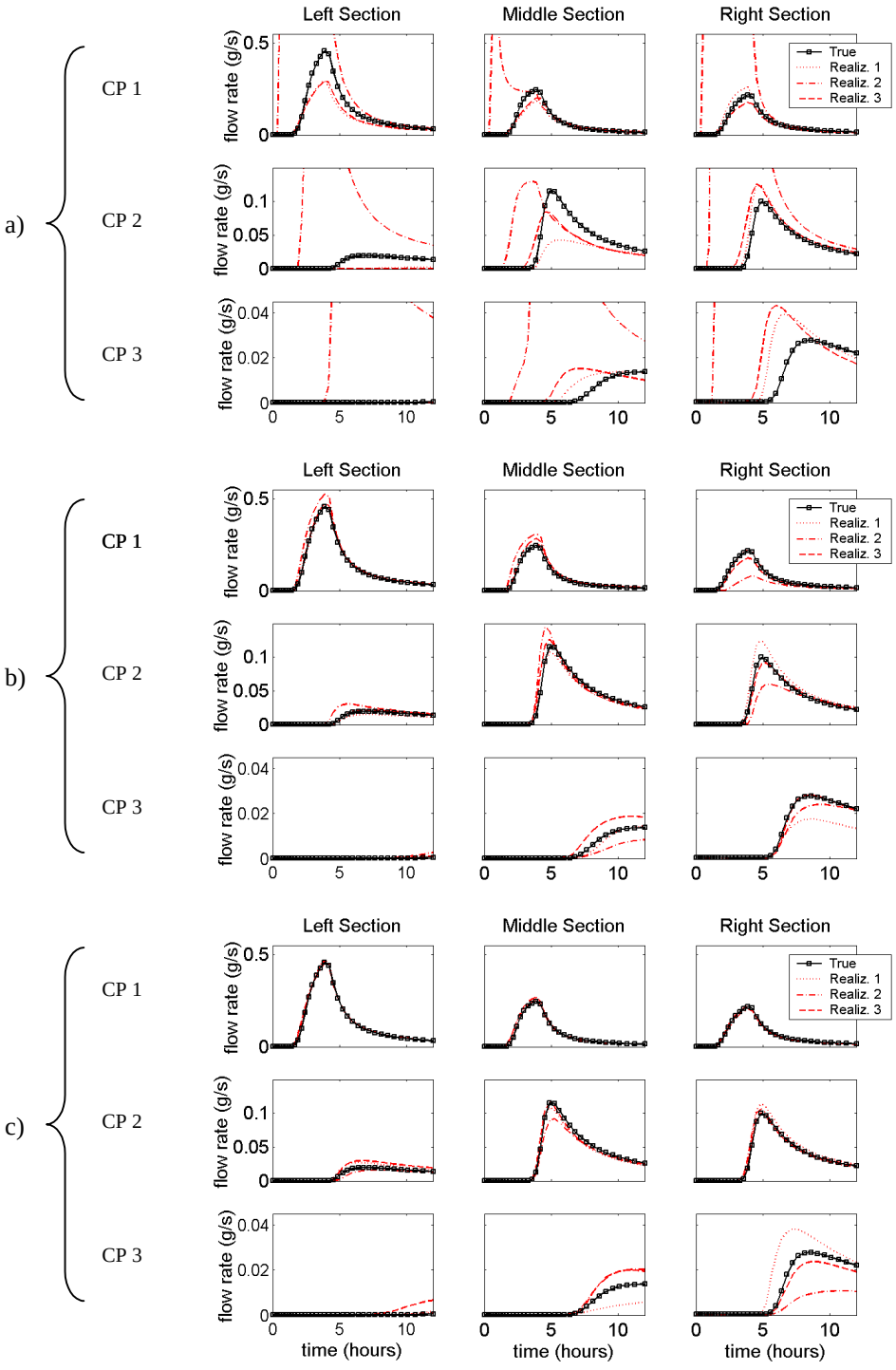

Figure 5. Breakthrough curves (total flow rates) for three sections of each control planes CP 1, CP 2, and CP 3 (as defined in Figure 1). Flow rate at each control plane is divided into the left section (1st column), middle section (2nd column), and right section (3rd column). Three cases are shown: a) conditional simulation; b) inversion using GPR; and c) inversion using GPR and borehole saturation values. Breakthrough for the true model is shown with black squares, and breakthrough for inversion using three different seed numbers (representing three realizations) are shown in red.